Pediatric Pathology

1867 Morphometric Study of Transition Zone in Hirschsprung's Disease Pull-Through Specimen Using Immunohistochemistry

Sanaz Ainechi, Suzanne Homan, Christine Sheehan, Hwa Jeong Lee. Albany Medical Center, Albany, NY.

Background: Incomplete resection of Hirschsprung's disease (HD) at the transition zone (TZ) may result in postoperative obstruction. However, histologic criteria of TZ are not well established. Recently, Calretinin has been suggested as an efficient tool to diagnose HD in mucosal biopsies. We utilized Calretinin and Peripherin, a novel but not quite validated marker for neurofilament of peripheral nervous system, to perform a morphometric study of TZ on pull-through specimens.

Design: Fourteen pull-through cases for HD were retrieved (2010-2014). Aganglionic zone (AG), TZ, and normal zone (NL) were mapped. The TZ was defined as the 3 cm zone proximal to the first appearance of submucosal ganglion cells. Representative tissue blocks from the three zones were stained for Calretinin and Peripherin. All H&E and immunostained slides were scanned by Nanozoomer Digital Slide System. The number of submucosal ganglia with hyperganglionosis (≥8 ganglion cells) was counted. The thickness of ten random submucosal and ten myenteric nerve plexuses were measured on digitalized slides (definition of 0.1 μm) at 20X resolution.

Results: The patients consisted of ten male and four female. Their ages ranged from 6 days to 39 months (mean age 4.5 months). The number of submucosal hyperganglionic ganglia was 3.6/cm in NL, and 2.1/cm in TZ (p=0.036). The submucosal nerve thickness did not show statistically significant difference between the TZ (average 27.49 μm) vs NL (average 24.95 μm). The submucosal nerve thickness was significantly thicker in AG (average 33.28 μm) compared to NL (p=0.025). All submucosal nerve plexuses in TZ were less than 40 μm. The thickness of myenteric nerve plexuses was highly variable independent of the zone. Both Calretinin and Peripherin highlighted ganglion cells, and myenteric and submucosal nerve plexuses. Calretinin was more sensitive in visualizing mucosal nerve fibers of TZ and NL compared to Peripherin. The degree of Calretinin immunostaining in the mucosal nerve fibers was not significantly different between TZ vs NL.

Conclusions: In pull-through specimens, the frequency of submucosal hyperganglionic ganglia may be used as a surrogate marker to identify TZ. Neither the thickness of the submucosal nerve plexuses nor the mucosal staining intensity of Calretinin can reliably distinguish TZ from NL. The performance of Calretinin and Peripherin is similar in detecting ganglion cells and nerve plexuses; however, Calretinin is more sensitive in visualizing mucosal nerve fibers.

1868 Comprehensive Genomic Profiling Reveals a High Frequency of Clinically Relevant Genomic Alterations in Neuroblastoma

Siraj Ali, Eric Sanford, Kai Wang, Matthew Hawryluk, Juliann Chmielecki, Julia Elvin, Roman Yelensky, Doron Lipson, Vincent Miller, Yael Mosse, Philip Stephens, John Maris, Jeffrey Ross. Foundation Medicine Inc, Cambridge, MA; Childens Hospital of Pennsylvania, Philadelphia, PA.

Background: Neuroblastoma (NB) arises from the sympathetic ganglion cells, and the most aggressive subset of these tumors metastasize and carry a high mortality for children. We reviewed 168 predominantly advanced, high-risk NB cases which underwent comprehensive genomic profiling (CGP) to identify clinically relevant genomic alterations (CRGA) that might allow for targeted therapeutic approaches .

Design: DNA was extracted from 40 microns of FFPE sections from 168 unique relapsed/refractory NB cases. Comprehensive genomic profiling (CGP) was performed on hybridization-captured, adaptor ligation based libraries to a mean coverage depth of >250X for the entire coding sequence of a minimum of 182 cancer-related genes plus 19 genes frequently rearranged in cancer. The results were evaluated for all classes of genomic alterations (GA). CRGA were defined as GA linked to drugs on the market or under evaluation in mechanism driven clinical trials.

Results: Patient characteristics: median age 6 (range 0 - 71 yrs); 100 males, 68 females. Specimens were sequenced to an average depth of 612x, and GA were present in 77% (129/168) of cases. These 168 cases harbored 244 GAs (1.5 alterations per tumor; range 0 to 7). 99 cases (59%) percent of cases harbored at least one CRGA, with a mean of 0.9 CRGAs per tumor (range 0 to 4). CRGAs in *MYCN* (38 cases; 22.6%) and *ALK* (28 cases; 16.7%, including 1 fusion gene) were identified, as well as GAs in *ATRX* (13 cases; 7.7%). Other CRGA include *CDK4* or *CDK6* amplification (12 cases, 7.1%), *RPTOR* amplification (7 cases, 4.2%), *HGF* amplification (5 cases, 3.0%), *FGFR1* base substitution (4 cases, 2.4%), and *BRAF* amplification (3 cases, 1.7%). One case harbored a novel *BEND5-ALK* fusion and the patient responded to crizotinib, and other patient responses to targeted agents will be presented.

Conclusions: CGP of 168 high-risk neuroblastoma cases led to the identification of CRGAs not assayed for as standard of care in this patient group. In particular, alterations in *ALK, CDK4/6*, *FGFR1*, *BRAF* and *mTOR* pathway genes are linked to targeted therapies currently approved or in development.

1869 Succsessful Experimental In Vitro MiTF Inhibition By Histone Deacetylase Inhibitors in a Massive Garment-Like Nevus – A Potential Treatment for Giant Congenital Melanocytic Nevi and Neurocutaneous Melanocytosis

Dipanjan Basu, Claudia Salgado, Marina Nikiforova, Bruce Bauer, Donald Johnson, Veronica Rundell, Miguel Reyes-Mugica. University of Pittsburgh School of Medicine, Pittsburgh, PA; North Shore University Health System, Northbrook, IL.

Background: Giant Congenital Melanocytic Nevi (GCMN) with brain/meningeal deposits characterize Neurocutaneous Melanocytosis (NCM). Neurologic symptoms portend a poor prognosis. These patients have increased risk of malignancy(<5%), and other severe complications. Somatic NRAS Q61 and BRAF V600E mutations occur in GCMN/NCM. No effective chemotherapy treatment is available. We describe the successful treatment *in vitro* of nevocytes from a massive GCMN/NCM.

Design: A Caucasian male was born with a GCMN massively involving his entire trunk, and multiple "satellite" lesions. Brain MRI showed characteristic NCM findings. Histology of the nevus resection was reviewed and fresh nevus samples were grown in primary cultures. DNA was extracted from nevus tissue, blood and cultured cells.

Results: Histology showed a GCMN with massive involvement of subcutis, dermis and dermoepidermal junction. IHC for melanocytic and neural crest cell markers (MiTF, CD56, DCT) were positive in histologic sections and cell cultures. PCR of DNA from nevus tissue, blood and cultured nevus cells showed heterozygous mutation of NRAS Q61K, confirming the NCM nature of the cultured cells. Primary cultures were treated with histone deacetylase inhibitor Trichostatin A (TSA). Cell survival was determined by MTT assay. TSA treatment suppressed MITF expression assessed by Western blot, and induced cell death in a dose dependent manner with an ED_{50} of 1μM.

Conclusions: HDAC inhibitors like TSA are able to induce cell death in NCM cells *in vitro*. Suppression of MITF expression by HDAC inhibitors could be an effective therapeutic approach against symptomatic NCM.

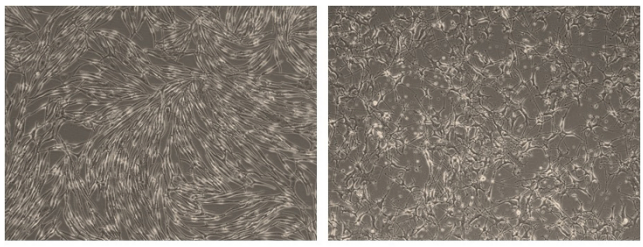

1870 H-RAS Mutation Is the Key Molecular Feature of Pediatric Bladder Cancer

Mireia Castillo-Martin, Ana Collazo Lorduy, Nataliya Gladoun, Grace Hyun, Carlos Cordon-Cardo. Icahn School of Medicine at Mount Sinai, New York, NY.

Background: Bladder cancer is a rare entity in the pediatric population making it difficult to define surveillance protocols and long term outcomes. Notably, almost all pediatric tumors are low grade and non-muscle invasive and do not recur. In order to explain the source of the different natural history between pediatric population and adults, we hypothesized that pediatric bladder cancer may potentially stem from different molecular pathways than its adult form. Our main objective was to study the most commonly altered genes in bladder cancer using mutational and immunohistochemical (IHC) analyses.

Design: Formalin fixed paraffin-embedded (FFPE) tissues of bladder tumors from three pediatric patients were retrospectively identified at the Columbia University pathology archives (1990-present) and re-evaluated. Clinical data was reviewed. DNA was extracted from the FFPE blocks with a Qiagen kit and the most well-known mutated spots of FGFR3 (exons 7, 10 and 15), H-RAS (exon 1), and PI3K (exons 9 and 20) were assessed by PCR amplification and Sanger sequencing. IHC analysis was performed using the standard avidin-biotin procedure with antibodies against p53, Pten, Rb, EGFR, Her2Neu to test their expression status. Finally, proliferative rate was assessed by Ki-67 IHC.

Results: Two patients had low-grade Ta bladder cancer, whereas the other tumor was classified as a Papillary Urothelial Neoplasm of Low Malignant Potential (PUNLMP). Two patients were female and one was male. The ages at diagnosis were 13, 11, and 17. None of the tumors recurred with a mean follow-up of 5.2 years (Range: 1.5-8.0 years). Interestingly, all the specimens showed H-RAS G12V mutation, whereas they were characterized by wild-type FGFR3 and PI3K. Nuclear p53 was not detected, while PTEN and Rb expression were diffusely maintained in the cytoplams and nucleus,

respectively. EGFR was homogenously expressed in the membrane of the tumor cells in the three cases, and Her2Neu was negative. The proliferation rate was very low in all cases (<5%).
Conclusions: Pediatric tumors arise from alteration of a pathway that is not initiated by the most commonly described FGFR3 or p53 mutations, but by H-RAS mutations. This distinction may explain the relatively few recurrences seen in the pediatric population. Molecular investigation of larger series of pediatric tumors is warranted, and will aid in determining the clinical follow up, if any, needed in this rare entity.

1871 Meconium-Associated Myonecrosis: Associations With Adverse Outcome and Placental Pathology

Adela Cimic, Rebecca Baergen. Weill Cornell Medical College, New York, NY.
Background: Intrauterine passage of meconium is common, occurring in approximately 10-15% of term births. Uncommonly, longstanding meconium may be associated with umbilical vascular myonecrosis and vasoconstriction. This under-recognized lesion has been associated with adverse perinatal outcome.
Design: This is a retrospective study of 481 placentas;139 with meconium-filled macrophages in the umbilical cord with associated myonecrosis (MMUNec), 139 with meconium in fetal membranes (MM), 62 with meconium in the cord without myonecrosis (MMU) and 139 controls without meconium (NoM) all of which were matched for gestational age (GA). We studied clinical and histologic factors including: clinical meconium (CM), Apgar scores (AS), fetal distress (FD), intrauterine growth restriction (IUGR), intrauterine fetal demise (IUFD), chorioamnionitis (CA), cord complications (CC), malperfusion (MP), thrombosis (FVT), chorangiosis (Chr) and nucleated red blood cells (NRBC). Median maternal age was 33.2 yrs; median GA was 39.4 wks. Data was analyzed by Chi-Square, ANOVA and Fisher exact test using SPSS software.

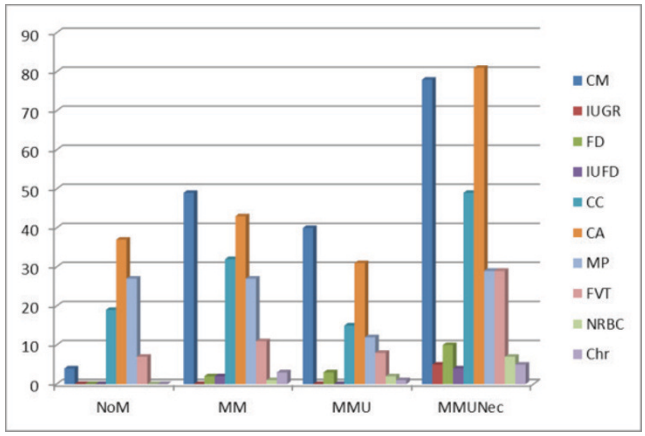

Results: MMUNec was significantly associated CM, FD, IUGR, IUFD, CA, CC, FVT, NRBC and Chr when compared to NoM ($p<0.05$). Compared to MM, only CM, FD, IUGR, CA, FVT, NRBC and Chr were significant. Interestingly, when compared to MMU, only CA retained significance. There was no difference between the groups in MP.

Compared to MMUNec	CM	IUGR	FD	CA	FTV	Chr	NRBC
NoM	0.001	0.023	0.001	0.001	0.001	0.023	0.007
MM	0.001	0.024	0.018	0.004	0.002	0.473	0.031
MMU	0.264	0.131	0.531	0.009	0.179	0.445	0.567

Conclusions: In conclusion, the finding of MMU or MMUNec, albeit subtle, is of clinical importance. A history of meconium discharge should trigger a meticulous search for MMU and particularly MMUNec. The latter is associated with adverse clinical outcome such as IUGR, IUFD, FD, low Apgar scores and placental lesions associated with hypoxia (NRBC and Chr). In addition, CA is significantly more common in all meconium groups compared to controls, which raises questions on the relationship of ascending infection to meconium discharge.

1872 Expression of FoxP3+ and ICAM-1 on Inflammatory Cells in Chronic Villitis

Erika Egal, Maria Heloisa Blotta, Harim dos Santos, Maria del Carmen Guillen, Fernanda Mariano, Albina Altemani. UNICAMP, Campinas, SP, Brazil.
Background: Placental chronic villitis has been associated with the transmission of infection between mother and fetus as well as with the maternal immune aggression of fetal tissues. In inflamed villi, most of the immune cells have been found to be of maternal origin. Intercellular adhesion molecule-1 (ICAM-1), a transmembrane glycoprotein, is expressed constitutively on the cell surface of a variety of cell types. The expression of ICAM -1 on the immune cell induces cell-cell adhesion allowing intercellular communication, T cell-mediated defense mechanism, and inflammatory response. On the other hand, regulatory T cells (Tregs), an immunosuppressive cell population, has been reported to be increased during pregnancy and it is important in allowing tolerance to the semi-allogenic fetus. The objective of this study was to quantify Treg cell population and ICAM-1 expression on immune cells in chronic villitis.
Design: We examined 10 cases of chronic villitis (all without an identifiable etiologic agent) using ICAM -1, CD45, CD3, CD68, and FoxP3 (the most specific marker of Treg cells) in serial tissue section. These cells were subdivided according to their location in inflamed villi: a) within the inflamed villi and b) outside the inflammed villi.
Results: Large amounts of CD45, CD3 and CD68 were found within the inflamed villi and forming perivillous aggregates attached to areas of trophoblastic loss. FoxP3+ Treg cells represented from 5% to 10% of immune cells and were observed mainly within the villi. The majority of immune cells surrounding areas of trophoblastic rupture showed marked expression of ICAM-1. In contrast, a small number of immune cells within the inflamed villi exhibited ICAM-1 expression.
Conclusions: In inflamed villi of chronic villitis, the level of ICAM-1 expression on immune cells depends on their location: high in number of cells in the perivillous region and low within the villi. Down-regulation of ICAM-1 on immune cells within the villi might be related to Treg cell presence, which could be maternal cells that react to fetal antigens and inhibit the immune response.

1873 Isochromosome 12p Analysis of Pediatric and Adult Sacrococcygeal Teratomas: Frequency and Evidence of Dual Histogenetic Pathways

Robert Emerson, Chia-Sui Kao, Mingsheng Wang, John Eble, David Grignon, Xiaoyan Wang, Shaobo Zhang, Rong Fan, Lawrence Roth, Timothy Masterson, Liang Cheng. Indiana University School of Medicine, Indianapolis, IN.
Background: Sacrococcygeal teratomas are rare tumors that occur most frequently in neonates, although adult cases also occur. The presence of immature elements in neonatal teratoma is not associated with malignant behavior. Coexisting nonteratomatous germ cell tumor, usually yolk sac tumor, is associated with poor prognosis. Few studies have evaluated the presence of overrepresentation of chromosome 12p in extragonadal germ cell tumors.
Design: 54 sacrococcygeal teratoma specimens from 52 patients were identified and available follow up information was obtained. The slides were reviewed to confirm the diagnosis and grade, using the ovarian teratoma grading system. Fluorescent in situ hybridization analysis was preformed to identify i(12p) abnormalities on paraffin blocks.
Results: Among the 48 pediatric patients, there were 44 teratomas and 4 tumors with teratoma and yolk sac tumor (1 of which also had primitive neuroectodermal tumor). The teratomas included 37 mature teratomas and 11 immature teratomas (4 grade 1, 2 grade 2, and 5 grade 3). The 44 teratomas lacking a yolk sac tumor component were all negative for i(12p). The 4 tumors with a yolk sac tumor component were all positive for i(12p). The 4 adult cases all lacked nonteratomatous germ cell tumor components, immature elements, and i(12p). Follow up information was available for 32 patients. Two patients with teratoma had recurrence, but were alive with no evidence of disease after long-term follow up. One patient with teratoma and yolk sac tumor had recurrence 7 months after resection. The other patients were alive with no evidence of disease at last follow up.
Conclusions: The i(12p) abnormality was not observed in the 4 adult sacrococcygeal teratomas. The i(12p) abnormality was detected in 8% (4/44) of pediatric sacrococcygeal germ cell tumors, but only in those with a nonteratomatous component. This is similar to the findings in ovarian teratomas with and without a nonteratomatous component. These cytogenetic findings suggest that pediatric sacrococcygeal teratomas should be considered two distinct groups, those with and those without other components, and that each group has a distinct molecular pathogenesis.

1874 Immunohistochemical Characterization of Inflammatory Infiltrates in Pediatric Chronic Cardiac Allograft Rejection

Alexander Gallan, M Kamran Mirza, Aliya Husain. University of Chicago, Chicago, IL.
Background: Approximately 250-300 pediatric heart transplants are performed annually worldwide. Chronic cardiac allograft rejection, also known as cardiac allograft vasculopathy (CAV), is a leading cause of graft loss and is characterized by coronary artery intimal thickening, luminal fibrosis, and endotheliitis. The risk of CAV development is significantly lower in pediatric vs. adult patients (15% vs. 50% at 5 years post-transplant). Mixed humoral and cell-mediated alloimmune response to the graft is thought to be a major pathogenic mechanism of CAV, however there is a paucity of data comparing the inflammatory infiltrate in pediatric and adult heart allografts. The goal of our study was to characterize the immunohistochemical composition of the intimal and perivascular inflammatory cells in pediatric vs. adult CAV.
Design: We identified all four post-mortem cases of CAV at our institution from 2005-2013 in orthotropic heart transplant patients under 21 years old who received standard triple immunosuppression and surveillance biopsies. Immunohistochemical stains for CD3, CD4, CD8, and CD20 were performed. Inflammatory infiltrates were identified as either intimal or perivascular, and the average number of cells per high power field (400X) staining positively for CD3 and CD20 were counted for both intimal and perivascular locations. The ratio of CD8+/CD4+ cells was also determined. Results were compared to those of the four most recent adult autopsy CAV cases.
Results: In pediatric patients, the intimal infiltrate contained an average of 80 CD3+ cells and 2 CD20+ cells per high power field. The ratio of CD8+/CD4+ cells was 1.89. The perivascular infiltrate contained an average of 182 CD3+ cells and 76 CD20+ cells per high power field. The ratio of CD8+/CD4+ cells was 0.97. In adult patients, the intimal infiltrate contained an average of 45 CD3+ cells and 1 CD20+ cells per high power field. The ratio of CD8+/CD4+ cells was 1.60. The perivascular infiltrate contained an average of 162 CD3+ cells and 123 CD20+ cells per high power field. The ratio of CD8+/CD4+ cells was 0.81.
Conclusions: Our results suggest that cell-mediated immunity plays a role in cardiac allograft vasculopathy, and that children and adults mount different inflammatory reactions to the graft. Compared to the adult patients, pediatric patients with CAV had a more robust intimal T cell response but a more modest perivascular B cell infiltrate. This may represent humoral immaturity in these younger patients and contribute to less allo-humoral damage and the lower rate of CAV seen in children.

1875 Association of Neuropeptide Y (NPY) and Its Receptors With Prognostic Factors and Survival in Neuroblastoma Patients

Susana Galli, Jason Tilan, Arlene Naranjo, Collin Van Ryn, Chao Yang, Jessica Tsuei, Emily Trinh, Joanna Kitlinska. Georgetown University Medical Center, Washington, DC.

Background: NPY is a neurotransmitter, abundantly expressed in neuroblastoma (NB). Previously, we have shown that NPY, acting via its Y2 receptor (Y2R), stimulates proliferation of NB cells and tumor vascularization, while inducible Y5 receptor (Y5R) promotes tumor cell survival and chemoresistance. The aim of the current study was to determine if NPY and its receptors correlate with prognostic factors in NB.

Design: We have tested matching samples of RNA, tissue sections and serum of 87 NB patients at various stages of the disease from the files of the Children's Oncology Group. The samples were analyzed in terms of the NPY system expression (NPY, Y2R and Y5R). Protein levels and mRNA in tumor were quantified by immunohistochemistry (IHC) and real time-PCR, respectively, while NPY in serum was measured by ELISA. The expression of other factors implicated in NB development and progression (MYCN, TrkA III, TrkB and BDNF) were detected on mRNA levels by real time-PCR. For each of the prognostic variables, a Wilcoxon rank-sum or Fisher's exact test were run to compare NPY and receptor values between groups and a log-rank test was performed to compare the event-free survival and overall survival.

Results: 1) NPY mRNA was detectable in 100% of analyzed tumors. IHC staining revealed that in differentiating and maturing cells NPY accumulated intracellularly, while in undifferentiated NBs the peptide was observed in extracellular spaces suggesting its free release. Serum concentrations of NPY were higher in NB patients with undifferentiated and poorly differentiated tumors, as compared to those with differentiating NBs (p-value=0.0308). High serum concentrations of NPY strongly correlated with several adverse prognostic factors (Stage 4, high risk, diploidy, and unfavorable prognosis) (p-value<0.03) and worse survival (p-value<0.04). 2) Y2R was expressed mainly in undifferentiated NB cells. mRNA of this receptor was detectable in 100% of cases and its levels positively correlated with MYCN expression 3) mRNA of Y5R was detectable in 84% of the tumors and correlated with expression of BDNF and its TrkB receptor, factors associated with poor prognosis. High NPY protein levels marked a population of invasive NB cells.

Conclusions: This study validated NPY and its receptors as targets for NB therapy. Serum NPY was the most highly prognostic variable, found to be associated with five of the NB prognostic factors. Higher NPY levels were correlated with the more detrimental value of the prognostic factors.

1876 High NPY Release Associates With Ewing Sarcoma Bone Dissemination – In Vivo Model of Site-Specific Metastases

Susana Galli, Sung-Hyeok Hong, Jason Tilan, Olga Rodriguez, Ewa Izycka-Swieszewska, Taylor Polk, Meredith Horton, Akanksha Mahajan, David Christian, Shari Jenkins, Rachel Acree, Phuong Ledo, Congyi Lu, Yichien Lee, Christopher Albanese, Joanna Kitlinska. Georgetown University Medical Center, Georgetown University, Washington, DC.

Background: Ewing sarcoma (ES) is a tumor of children and young adults that develops in bones and soft tissues. The presence of metastases, particularly with bone involvement, is the most adverse prognostic factor. However, the mechanisms governing formation of such metastases are unclear, while lack of clinical material and appropriate animal models hinders studies aiming at their identification. Neuropeptide Y (NPY) is a transcriptional target of EWS-FLI1, the fusion protein that drives ES malignant transformation. NPY is highly expressed and released from ES tumors. Hypoxic tumor environment further increases NPY expression and activates its pro-metastatic functions, suggesting its role in ES dissemination.

Design: To test this, two ES cell lines, NPY-rich SK-ES1 and TC71, which does not secrete the peptide, were used in orthotopic xenograft model mimicking ES progression. ES cells were injected into gastrocnemius muscles of SCID/beige mice, primary tumors excised and mice monitored for the presence of metastases. Both cell lines gave rise to primary tumors with local bone invasion, yet varied in the patterns of their distant metastases.

Results: TC71 xenografts metastasized to the lungs (70%) and gave rise to local relapses (92%). In contrast, mice injected with SK-ES1 cells presented with extraosseous metastases to thoracic region (67%), dissemination to bones (50%) and brain (25%). Primary cells isolated from SK-ES1 metastases had increased growth rate and metastatic potential upon re-introduction to the animals. The high frequency of bone metastases observed in NPY-rich SK-ES1 cells suggested the role for the peptide in ES bone invasion. This was supported by increased NPY expression in bone metastases and its accumulation in the tumor tissue adjacent to the bones.

Conclusions: The metastatic patterns observed closely resemble metastatic sites in ES patients confirming clinical relevance of our model. Moreover, our results further support the role of NPY in ES biology and its potential involvement in dissemination and bone invasion. Understanding the mechanisms of NPY actions in ES may have implications for other NPY-rich malignancies and can be used to identify pathways driving ES metastases to the specific niches and to test therapeutics targeting them.

1877 ROR2 Is a Highly Expressed Biomarker and Potential Therapeutic Target in Wilms Tumor

Jenny Hoffmann, Sushama Varma, Patricia Robison, Inigo Espinoza, Matt Van de Rijn. Stanford University Medical Center, Stanford, CA; Hospital de la Santa Creu i Sant Pau, Autonomous University of Barcelona, Barcelona, Spain.

Background: Wilms tumor (WT), or nephroblastoma, is the most common pediatric renal malignancy, with propensity for local recurrence and metastasis for which currently there is no targeted therapy. Receptor tyrosine kinases (RTKs) have been shown to play a role in a variety of cancers, such as the targeting of HER2 in breast cancer by monoclonal antibodies. ROR2 is a membrane-bound RTK which has recently been shown to be expressed in several malignancies, and has been found to have a pro-tumorigenic effect using in vitro and xenograft models. ROR2 is also expressed in the metanephric mesenchyme of the embryonic kidney, the histomorphology of which is recapitulated by WTs. The role of ROR2 in WT has yet to be described in the literature.

Design: A retrospective search of the surgical pathology database of Stanford University Medical Center identified 65 cases of WT from 48 patients between the years of 1995-2011, including 46 primary kidney tumors, 8 local recurrences, and 11 metastases. H&E stained sections were reviewed and immunohistochemistry was performed for ROR2 on each tumor. We additionally assessed ROR2 protein expression in developing human fetal kidneys specimens between 12-24 weeks gestational age. Membranous staining was scored as negative, equivocal, weak, or strong.

Results: Of the 65 tumors, 62 showed expression of ROR2. Strong ROR2 expression was seen in 41 tumors, and weak ROR2 expression was seen in 21 tumors. The staining was predominantly seen in the blastemal areas with epithelial structures showing variable staining. Stromal areas were mostly negative. Evaluation of ROR2 immunohistochemical stains in normal fetal kidneys showed that strong ROR expression is seen at 12 weeks gestational age, and decreases in intensity until it is negative by 24 weeks gestational age.

Conclusions: ROR2 is expressed in the normal fetal kidney in the earlier stages of development, and is later down regulated. ROR2 is also highly expressed in a significant percentage of WTs, and may function as a potential therapeutic target.

1878 Role of Rapid Improvised Acetylcholinesterase Histochemistry in the Diagnosis of Hirschsprung's Disease: A 14-Year Prospective Study of 1890 Rectal Biopsies at a Referral Centre in India

Usha Kini, Manjaly Babu, Suravi Mohanty, P Divya, Kanishka Das, BN Nandeesh, Lokendra Yadav. St.John's Medical College and Hospital (SJMCH), Bangalore, India.

Background: The introduction of laparoscopic and transanal endorectal pull through surgeries, revolutionized the operative procedures for Hirschsprung disease (HD) and demanded rapid diagnostic modalities for pre-operative and intra-operative purposes. A 14 year prospective study of rectal biopsies for suspected HD using rapid improvised acetylcholinesterase (AChE) histochemistry technique standardised in our laboratory (the only referral diagnostic centre for HD in India) is a great boon to the pediatric population in developing countries.

Design: 1890 pediatric rectal mucosal biopsies (from 1200 suspected HD patients) and 154 leveling doughnuts (proved HD) during the 14 year period (2000-to date) were processed by our improvisation of modified Karnovsky's and Roots method of AChE histochemistry on non-snap frozen cryo-sections (staining time 30 minutes). Every case was evaluated by four investigators.The data was analysed using standard statistical packages. The Institutional Ethical Committee approval was obtained.

Results: HD was confirmed in 422 (35%) cases giving an overall incidence of 1:2000 live births in south India. They were further classified based on the length of aganglionosis [rectosigmoid 377 (90%), long segment 22 (5%), and total colonic aganglionic 20 (5%)]. Biopsies diagnosed as HD showed positive AChE fibers stained black with demonstrable mucosal patterns (57%, 32% and 11% of A, B and Equivocal patterns respectively). 130 inadequate biopsies were diagnosable with AChE and so were the low level biopsies as ratified by Calretinin immunohistochemistry. Extra care was needed in the interpretation of 114 (27%) biopsies from neonates as the AChE fibers were fewer and less thick. Four false positive cases due to over incubation during staining were identified by lack of correlation with clinical presentation and sorted by repeat staining. 24(16%) doughnuts sampled during anastomosis showed abnormal innervation involving more than one quarter necessitating a second doughnut examination more proximally.

Conclusions: The rapid improvised AChE staining on non- snap frozen sections of rectal biopsies for diagnosing HD is user friendly, economical, with faster TAT, 100% specificity and near 100% sensitivity. Even low level and inadequate biopsies turned to be diagnostic with this technique. Hence our improvised AChE histochemistry technique has helped to make primary intraoperative diagnosis of HD and thus save colons in 65% of children suspected of HD.

1879 Erythroid Gene Expression in Diamond-Blackfan Anemia

Cassie Lee, Elizabeth Moschiano, Paul Pattengale, Matthew Oberley. Children's Hospital Los Angeles, Los Angeles, CA.

Background: Diamond-Blackfan Anemia (DBA) is a congenital ribosomopathy characterized by reticulocytopenia, macrocytic anemia, and a predisposition to malignancy. In 60-70% of patients, somatic mutations in 11 genes involved in ribosome biogenesis underlie the clinical phenotype. It is not clear why these mutations specifically affect the erythroid lineage. Somatic mutations in GATA1 have been identified in rare cases of DBA which result in decreased GATA1 protein levels. It was shown that GATA1 expression was also decreased in DBA patients with RBS19 mutations, suggesting a mechanism for the specific erythroid defect. To further characterize the specific erythroid defect, we have examined the immunophenotypic expression of erythroid antigens in erythroid precursors (EP) in DBA patients.

Design: Cases of DBA were identified from the files of Children's Hospital of Los Angeles (CHLA). All patients had macrocytic anemia, reticulocytopenia, and severe erythroid hypoplasia in the diagnostic bone marrow evaluation. Immunohistochemical (IHC) evaluation of E-Cadherin, CD71, Hemoglobin A, and Parvovirus B19 was performed. GATA1 IHC assessment of the bone marrow biopsies is currently in progress.

Results: 7 patients were identified from CHLA; 6 male and 1 female. The median age of patients at diagnostic biopsy was 7.4 months (+/- 5.5), and the median length of followup was 147 months (+/- 74; 2 patients lost to followup). Of patients for which data is available, only 1/5 improved with steroid treatment, while 4/5 required lifelong transfusion. 1 of 2 patients who received a BMT died of transplant related complications.

1 of 5 patients developed a secondary malignancy (osteosarcoma). Bone marrow aspirate findings showed a median of 0.3% (+/-0.3) EP at diagnosis. Mean lymphoid component was markedly increased at 44.4% (+/-10.5). Bone marrow biopsy confirmed erythroid hypoplasia in 7/7 biopsy sections examined. IHC showed E-cadherin staining of EP in all 7 cases providing a means for quantitation. All of the bone marrow biopsies showed significantly less than 1% EP except in the steroid responsive patient who had 3-5% EP. IHC for CD71 identified slightly fewer EPs, while Hemoglobin A was largely negative. Parvovirus IHC was uniformly negative in all patients.
Conclusions: 1. Evaluation of EP marker expression suggests E-cadherin is the ideal marker to quantitate erythroid precursors in patients with DBA. 2. The patient responsiveness to steroids may be related to the quantity of EP present in the bone marrow at diagnosis. 3. Patients in our DBA series all uniformly had an increased lymphoid component.

1880 Role of CIC-DUX4 and BCOR-CCNB3 Fusions in Redefining Pediatric Undifferentiated Sarcoma (UND) and Translocation Negative Ewing Sarcomas (ES)

Kathrin Ludwig, Patrizia Dall'Igna, Gianni Bisogno, Rita Alaggio, Angelia Zin. University of Padua, Padua, Italy; Institute of Pediatric Research (IRP), Città della Speranza, Padua, Italy.
Background: Ewing sarcomas are primitive round cell tumors of bone and soft tissue of uncertain histogenesis. They are characterized by recurrent balanced translocations involving EWSR1 gene and members of the ETS gene family. Recently, a sub-group of UND with Ewing-like features and specific transcripts has been identified. CIC-DUX4 and BCOR-CCNB3 fusions have been detected in 68% and 4% of UND respectively. Whether they represent variants of ES, or distinct entities is so far unknown. In this study we investigated the presence of these transcripts in a series of pediatric sarcomas with histological characteristics of ES or UND.
Design: 284 pediatric cases (age range 0.5-18 yrs) with histological diagnosis of ES or UND were analyzed by reverse-transcriptase polymerase chain reaction (RT-PCR) assays to specifically detect *EWS/FLI1, EWS-ERG and EWS/ETV4* transcripts in fresh-frozen and formalin-fixed, paraffin-embedded tissues. Tumors negative for all analyzed translocations underwent RT-PCR for CIC-DUX4 and BCOR-CCNB3 fusion transcripts.
Results: 264 (93 %) Ewing/PNET sarcomas harboured one of the classical EWSR1-ETS-family translocations. Of the 20 translocation negative cases one (0.4%) ES had a CIC-DUX4 fusion, whereas 2 UND (0.7%) harboured the BCOR-CCNB3 transcript. These two tumors showed a heterogeneous morphology, with elongated cells suggestive of a malignant peripheral nerve sheath tumor in one and a frankly round cell morphology with chondroid areas in the other, reminiscent of mesenchymal chondrosarcoma. The CIC-DUX4 sarcoma was composed of elongated cells with a clear cytoplasm and occasional nest formation. Immunostains were non contributive. CD99 was positive in the CIC-DUX4 and one of the BCOR cases.
Conclusions: CIC-DUX4 and BCOR-CCNB3 sarcomas should be considered in the spectrum of differential diagnoses of pediatric UND. These molecular investigations should be included in the diagnostic work-up of these tumors. Moreover, the morphologic heterogeneity of BCOR sarcomas may represent a diagnostic pitfall, simulating MPNST and mesenchymal chondrosarcoma, like in our cases.

1881 Can Morphological and Clinical Features in Post Therapy Neuroblastic Tumors Predict Recurrence?

Vikas Mehta, Shakeel Modak, Hikmat Al-Ahmadie, Anuradha Gopalan, Sahussapont Sirintrapun, Yingbei Chen, Samson Fine, Victor Reuter, Satish Tickoo. Memorial Sloan Kettering Cancer Center, New York, NY.
Background: Low- and intermediate-risk neuroblastomas (NB) have >90% survival rates, while high-risk NBs are frequently chemo- and radio-therapy resistant, often resulting in treatment failure and recurrence. Morphological features and therapy-related changes in post-therapy neuroblastic tumors (PTNB) are generally regarded as unreliable for prognostication. Only rare studies have addressed this subject, mostly based on small number of cases. The aim of this study was to explore the potential association of morphological features with outcome/recurrence in a large series of cases of PTNB with resection at a single institution.
Design: We reviewed 199 cases of PTNB, surgically resected at our institution from 2005 to 2010. For the purpose of this study, PTNBs were classified using International Neuroblastoma Pathology Classification criteria for therapy-naïve NB. This cohort was subdivided into 2 groups: patients with subsequent recurrences and those without. Multiple pathological features (Table 1) were evaluated. Statistical tests were performed to evaluate association of clinical and pathological parameters with recurrence.
Results: Results are as follows:

PARAMETER	NO RECURRENCE (n=137)	RECURRENCE (n=62)	p-value (univariate analysis)	p-value (multivariate analysis)
M:F ratio	0.9:1	1.5:1	0.24	
Age in years (mean)	0.5-14(3.7)	0.7-27(5.9)	0.0009	NS
Residual mass size on pathological examination in cm (median)	0.7-18(4.5)	0.6-19.5(5.3)	0.10	
Lymphovascular invasion (LVI)	35(25%)	33(54%)	0.0003	0.0005
Lymph node metastasis	97(71%)	53(86%)	0.023	NS
MYCN amplification	19(14%)	13(21%)	0.22	
% Treatment response, range (mean)	10-100(52)	5-100(48)	0.26	
Mitosis-Karyorrhexis index (MKI) (intermediate and high)	18(13%)	14(23%)	0.009	0.036
NB-MOR	47(34%)	36(58%)	0.002	0.002
Margin positive	15(24%)	22(16%)	0.19	

NS=not significant; NB-MOR=Post-therapy neurobalstic tumor morphology, including undifferentiated (U)/poorly differentiated (PD) NB, nodular ganglioNB with U/PD histology. Additionally, 3/3 cases with anaplastic pleomorphic morphology developed recurrence.

Conclusions: A significant association between development of recurrence and presence of LVI, intermediate/high MKI and post therapy tumor morphology is seen in PTNBs. Our findings indicate that detailed evaluation of PTNBs, similar to that performed on pre-therapy NBs, provides important prognostic information and should be detailed in pathology reports on such residual tumors.

1882 Association of Increased Baseline D-Dimer With Incidence of Thrombosis Based on Autopsy Findings in Pediatric Patients on Extracorporeal Membrane Oxygenation

Christina Otterness, Esther Soundar, Karen Eldin, Jun Teruya. Baylor College of Medicine, Houston, TX; Texas Children's Hospital, Houston, TX.
Background: Pediatric patients requiring extracorporeal membrane oxygenation (ECMO) are at increased risk for serious bleeding and/or thrombosis. The extracorporeal circuit provides a massive surface area that may activate the coagulation system therefore patients on ECMO routinely receive anticoagulation. Although coagulation parameters are closely monitored while on ECMO, their derangement is obvious only when a disastrous hemorrhagic or thrombotic event occurs. However, it would be a great benefit if laboratory test(s) could predict hemostatic alterations and alert clinicians of impending hemorrhage or thrombosis.
Design: A retrospective chart review was performed to identify patients that died while receiving ECMO or within 24 hours of the discontinuation of ECMO and had an autopsy performed between 2006 and 2014 at a single pediatric hospital. Demographic and clinical variables, baseline and post-initiation clinical lab data including PT, PTT, fibrinogen, D-dimer, platelet count, anti-Xa, antithrombin, and plasma free hemoglobin were extracted from the electronic medical records. The autopsy reports were reviewed to identify any organ(s) that had evidence of thrombosis or hemorrhage. Non-parametric analysis was done to evaluate the association between the laboratory variables with hemorrhage or thrombosis.
Results: Thirty patients [age 0.46 years (0.08-3.41), males 16 (53.3%)] were identified and of these, 29 patients (97%) were noted to have hemorrhage in at least one organ system on autopsy. Thrombosis was identified in 17 (57%) of the patients. Thrombosis was associated with hemorrhage in 16 of 17 cases (94%). Laboratory data in patients with thrombosis compared to patients without thrombosis showed increased baseline D-dimer levels [7.63 μg/mL (2.49-20.00) vs 1.85 (1.59-2.14) p=0.02], lower post-initiation anti-Xa levels [0.18 units/mL (0.13-0.38) vs 0.46 (0.21-0.98) p=0.08], and higher plasma free hemoglobin during ECMO [40.35 mg/dL (20.20-117.20) vs 18.28 (10.98-43.98), p=0.06].
Conclusions: An increased baseline D-dimer level may be a risk factor for thrombotic complications during ECMO. Patients with thrombosis also tended to have increased plasma free hemoglobin levels and lower post-initiation anti-Xa levels, but without reduced organ hemorrhage at autopsy.

1883 Expression of ABCB1, ABCC1 and ABCG2 Transporters on 40 Retinoblastomas Cases Naive To Chemotherapy Treatment

M Ponce, Blanca Castro, Adriana Hernandez, Guillermo Ramon, Eunice Aguilar, Javier Camacho, Manuela Orjuela, Stanislaw Sadowinski, Ma de Lourdes Cabrera. IMSS, México, DF, Mexico; CINVESTAV, México, DF, Mexico; Columbia University, New York, NY; Hospital Infantil de México Federico Gómez, México, DF, Mexico.
Background: One of the most important mechanisms involved in chemotherapy failure in cancer is Multi Drug Resistance (MDR). ABC transporters constitute a superfamily of molecular pumps that efflux metabolites, xenobiotics and drugs outside the cell. ABCB1, ABCC1 and ABCG2 are ABC transporters discovered because they confer resistance to antineoplastic molecules in cultured tumor cells. In many types of malignant tumors some of those transporters are overexpressed causing chemotherapy failure and thus tumor progression. Eventhough expression of these transporters has been well studied

in many types of adult tumors, expression of ABC transporters and correlation with clinical features have been scarcely reported in retinoblastoma, an intraocular malignant tumor occurring mainly in early infancy.
Design: The aim of this work was to determine mRNA expression of ABCB1, ABCC1 and ABCG2 by qRT-PCR in retinoblastoma and to explore whether or not correlations with relevant clinical features do exist. To do this, we isolated RNA from 40 untreated retinoblastoma briefly cultured for one week after enucleation including 20 unilateral and 20 bilateral cases. To test whether mRNA levels correlate with the corresponding protein expression, we also did immunohistochemistry for ABCB1 and ABCC1 in representative cases.
Results: We found an overall higher mRNA expression of ABCC1 followed by ABCB1 and negligible expression of ABCG2. Segregation of expression data by laterality shows no difference in ABCB1 expression, in contrast ABCC1 expression is moderately higher in bilateral cases and the expression data spreads on a larger interval revealing tumor heterogeneity. Segregation of expression data by clinical stage of tumors do not show any association either. The expression of qRT-PCR data is inconsistent with immunohistochemical findings.
Conclusions: From the three transporters studied, we detected mRNA from ABCB1 and ABCC1 in all retinoblastoma studied. In bilateral cases expression of ABCC1 is higher, however immunohistochemical findings are inconsistent with RNA data, at least, with the antibodies used.

1884 Utility of Clinical High-Depth Next Generation Sequencing for Somatic Variant Detection: Application To PIK3CA Variant Detection in Segmental Overgrowth Related Syndromes

Archana Shenoy, Vishwanathan Hucthagowder, Dorothy Grange, Catherine Cottrell. Washington University School of Medicine, St. Louis, MO.
Background: Next-generation sequencing (NGS) has demonstrated clinical utility in applications such as tumor genetic profiling for detection of somatic alterations. Due to tumor/normal admixture and subclonality, a high depth of sequence reads is required for adequate assay sensitivity. Increasingly post-zygotic (somatic) alterations are a recognized cause of congenital disorders. Somatic overgrowth (SO) related syndromes are associated with activating mutations of the PI3K-AKT pathway including *AKT1, AKT2, AKT3*, *MTOR, PIK3CA,* and *PIK3R2*. Somatic alterations within the *PIK3CA* gene are associated with megalencephaly-capillary malformation (MCAP) and congenital lipomatous asymmetric overgrowth of trunk, vascular malformations, epidermal nevi and skeletal anomalies (CLOVES). The resultant mosaicism is not reportedly detected in peripheral blood (PB) and necessitates analysis of disease involved tissues. Due to low observed variant allele frequency (VAF), a sensitive assay such as high depth NGS is necessary for variant detection. Here we present the utility of clinical NGS in detecting *PIK3CA* mutations in three patients with SO.
Design: Paired-end 101bp NGS was performed using target-hybrid capture with an average unique on-target platform depth of 1000x. Sequence variants were called using GATK v1.2. Sequenced specimens included PB (patient 1), buccal (patients 1,3), and fresh lipomatous soft tissue (LT) (patients 2,3). Patients 1 and 2 carried a diagnosis of MCAP and patient 3, CLOVES.
Results: *PIK3CA* mutations were detected in all patients. Patient 1 harbored a p.P104L alteration with a VAF of 37% in buccal and <1% in PB. Patient 2 harbored a p.E545D alteration in LT at <10% VAF, and patient 3 harbored a p.C420R alteration in LT at 29% VAF which was not detected in buccal. The p.P104L variant was novel in the setting of SO, whereas p.E545D and p.C420R have been previously described.
Conclusions: As in a cancer setting, mutations in SO are associated with low VAF necessitating high-depth NGS for genetic analysis. Using this approach PIK3CA mutations were identified in 3 patients with SO. Tissue specific mosaicism was observed, and these results corroborate the need to sequence disease involved tissue. The clinical applications for somatic variant detection are expanding along with the potential of gene targeted therapeutics in the future.

1885 Transaldolase-1 Immunohistochemistry: A Useful Screening Tool To Diagnose Transaldolase Deficiency in Liver Specimens

Maryam Shirazi, Mercedes Martinez, Jay Lefkowitch, Marcela Salomao. Columbia University Medical Center, New York, NY.
Background: Transaldolase (TAL) is a key enzyme in the non-oxidative phase of pentose phosphate pathway (PPP). TAL deficiency is an autosomal recessive disorder with a wide range of non-specific manifestations including growth retardation, myocardial hypertrophy, and neonatal liver disease ranging from steatosis to cirrhosis to early development of hepatocellular carcinoma. In these cases, the identification of liver disease often involves liver biopsy. The diagnosis of TAL deficiency relies on laborious techniques, including urine biochemical analysis followed by genetic analysis of the TALDO1 gene. TAL immunohistochemistry (IHC) has been widely used in animal studies and anti-human TAL antibodies are commercially available. However, its usefulness in diagnosing TAL deficiency in liver specimens has not been described. In this study, we describe the usefulness of TAL IHC in identifying TAL deficiency.
Design: With IRB approval, three TAL-deficient liver samples (two liver biopsies and one liver explant) and ten normal liver controls were obtained from our surgical pathology archives. TAL-deficient cases were siblings who were previously diagnosed by whole exome sequencing. Following antigen retrieval in ULTRA Cell Conditioning Solution (ULTRA CC1), slides were stained with anti-transaldolase antibody (rabbit polyclonal Ab, dilution 1:100, Abcam, Cambridge, MA) on an autostainer (Ventana Benchmark Ultra, Tucson, AZ).
Results: TAL immunohistochemistry of control cases resulted in strong nuclear and weak cytoplasmic staining of the hepatocytes. In contrast, TAL immunohistochemical staining was negative in all three cases with TAL deficiency.
Conclusions: TAL immunohistochemistry successfully identified cases of TAL deficiency. This approach offers a quick and inexpensive screening tool in the subset of pediatric patients with liver disease of unknown etiology.

1886 Maternal Metabolic Abnormalities and Dynamic Ablative Site Placental Remodeling in Twin-To-Twin Transfusion Syndrome With and Without Selective Fetoscopic Laser Photocoagulation (SFLP)

Sarah Starnes, Philip Fitchev, Constance Thorpe, Emanuel Vlastos, Suwan Mehra, Mona Cornwell, Susan Crawford. Saint Louis University School of Medicine, St. Louis, MO.
Background: Twin-to-twin transfusion syndrome (TTTS), an often fatal complication of twin pregnancy affecting up to 15% of monochorionic diamniotic twin pregnancies, results from an unequal sharing of blood across placental vascular anastomoses between twins. The current therapy of choice for TTTS is selective fetoscopic laser photocoagulation (SFLP) and interruption of anastomoses. After SFLP, TTTS recurrence affects up to 16% of cases and heralds a poor outcome. Previous work in the area of TTTS placental pathology has focused largely on angioarchitecture exclusive of SFLP treatment.
Design: Case histories were gathered on monochorionic twin placentas from women with high-risk twin gestations (n=38); 28 cases were treated by SFLP for TTTS (n=22) and associated conditions and 10 were untreated. All placentas were evaluated by gross and microscopic evaluation, including ex vivo vascular injection studies. Areas distant from and at SFLP sites were sampled for microscopic evaluation. Additional studies included immunohistochemistry (IHC) to assess the evolution of vascular and metabolic changes after SFLP (VEGF, PEDF).
Results: Within the cohort, there was a higher than expected rate of co-morbidities such as obesity, diabetes, and smoking. Several placentas were small for gestational age (14% of those without remote IUFD). There was abnormal umbilical cord insertion in most cases (68%). Intravascular calcifications were commonly present in cases both with and without SFLP. Within hours or days after SFLP, cases showed early wedge infarcts with necrosis (4/22). There were remote wedge infarcts and a stippled border of calcification days to weeks after SFLP (6/22). Many weeks later, chorionic vessels at SFLP sites displayed remodeling and medial hypertrophy (8/22). There was a relative increase in expression of the pro-angiogenic factor VEGF in TTTS chorionic villi, but antiangiogenic factor PEDF was relatively low.
Conclusions: In this cohort of women with TTTS-affected pregnancies, metabolic co-morbidities were prevalent (61%), suggesting an association between TTTS development and abnormal maternal metabolism. The vascular changes associated with SFLP sites over time show that while superficial, ablation by SFLP yields dynamic vascular adaptation rather than static disrupted perfusion. Disparate VEGF and PEDF expression reflect a pro-angiogenic phenotype in TTTS vasculature.

1887 Whole Slide Imaging for Diagnosis of Pediatric Tumors and Tumorous Lesions: Experience in a Large Tertiary Care Hospital in Saudi Arabia

Wajiha Sufyan, Mohammad Ashraf Ali Aziz, Hanaa Bamefleh, Hesham Musleh, Walid Khalbuss. National Guard Health Affairs- King AbdulAziz Medical City, Riyadh, Saudi Arabia.
Background: In the recent years there has been an increasing trend in utilization of the Whole slide imaging (WSI) technology in pathology practice. WSI has been successfully used in education; research; image analysis; for primary diagnosis as well as in consultations and quality assurance. The aim of this study is to test the practicality and feasibility of using WSI in diagnosis of Pediatric tumors and tumorous lesions.
Design: Sixty tissue biopsies (core as well as excisional) and resections from patients less than 15 years old were selected from 2011 to 2014 from the Pediatric Hemato-oncology, and Pediatric surgery multidisciplinary team meetings cases with wide spectrum of diagnoses. These cases had been diagnosed by multiple pathologists in our institution. Three pathologists reviewed the formalin fixed paraffin embedded tissue sections of the cases using WSI technology at 20X magnification. Then, after a washout period of 2 weeks the three pathologists reviewed the same cases using light microscopy. The original clinical information was available, but they were blinded to the primary light microscopic diagnosis and interpretation. The WSI based diagnoses were compared with light microscopy diagnoses and classified as concordant, mildly discordant (without clinical implications) and discordant (with clinical implications).
Results: Different outcomes of WSI and Glass Slides for diagnosis of Pediatric tumors and tumorous lesions are shown in Table 1.

Different Outcomes of WSI and Glass Slides for Diagnosis of Pediatric Tumors and Tumorous Lesions	
Accuracy of WSI	90.5 %
Accuracy of Glass Slides	92.3 %
Concordance between WSI and Glass Slides	94.0 %
Discordance between WSI and Glass Slides	6.0 %
Concordance and minor discordance between WSI and Glass Slides	96.5 %

Conclusions: Diagnosis of Pediatric tumors and tumorous lesions may be done using WSI within an acceptable range of diagnostic accuracy. Some difficulties that can be encountered in the assessment may overcome by scanning at higher magnification (x40 instead of x20) and possibly by using Z-stack function. We believe that with further training and improving of WSI technology, it might be possible to implement WSI in diagnosis of pediatric lesions.

1888 Role of von Willebrand Factor Sequestration and Glycoprotein 1b Expression in Wilms Tumor-Associated Acquired von Willebrand Syndrome: An Immunohistochemical Study

Alexander Thurman, Jamal Benhamida, Scott Kogan. University of California, San Francisco Medical Center, San Francisco, CA.

Background: Acquired von Willebrand syndrome (AvWS) represents an acquired quantitative or qualitative defect in von Willebrand factor (vWF) that may result in clinical bleeding. AvWS is known to be associated with various disease states, including myeloproliferative disorders, paraproteinemias, solid tumors, autoimmune disorders, and hormonal alterations. Specifically, AvWS has been well-described in pediatric patients with Wilms tumor (WT). The incidence of this complication is high, with estimates of laboratory-confirmed AvWS ranging from 8 to 30 percent. The pathogenesis underlying this association is unknown, although mechanisms involving secreted hyaluronic acid and/or sequestration of vWF by tumor cells have been proposed. We herein present (1) the largest immunohistochemical study to date of surface vWF labeling in WT and (2) to our knowledge, the first study to explore a potential etiologic link between WT and AvWS—namely, the expression of glycoprotein 1b (GP1b), a component of the canonical vWF-binding GP1b-9-5 surface receptor complex, by WT cells.

Design: We retrospectively collected 28 cases of WT and 26 control cases from the archived clinical specimens of the Department of Pathology at the University of California, San Francisco Medical Center. Control cases consisted of 16 clear cell renal cell carcinomas (RCCs), 5 papillary RCCs, 2 chromophobe RCCs, 2 clear cell papillary RCCs, and 1 rhabdoid tumor of kidney. AvWS-related clinical and laboratory data were obtained for all patients. Immunohistochemical (IHC) staining for both vWF and GP1b were performed on all cases at ARUP Laboratories (Salt Lake City, Utah).

Results: 7 of 28 patients with WT (25%) experienced clinical bleeding episodes which were suspicious for a bleeding diathesis. AvWS laboratory parameters were available in only 1 WT patient with clinical bleeding but were not diagnostic for AvWS. Tumor cells from WT and control cases did not exhibit membranous staining with either vWF or GP1b. Patchy, nonspecific cytoplasmic staining for vWF was noted in a minority of cases, predominantly occurring in stromal cells.

Conclusions: Our results are consistent with prior immunohistochemical and indirect immunofluorescence studies of vWF labeling performed on clinical samples from patients with WT and AvWS. Lack of staining with both vWF and GP1b provides compelling evidence against a role for vWF sequestration or aberrant GP1b expression in the pathogenesis of WT-associated AvWS.

1889 Histologic Features of Intestinal Thrombotic Microangiopathy (iTMA) After Hematopoietic Stem Cell Transplant (HSCT)

Mikako Warren, Javier El-Bietar, Christopher Dandoy, Kasiani Myers, Adam Lane, Stella Devies, Sonata Jodele. Cincinnati Children's Hospital, Cincinnati, OH.

Background: We showed post-transplant TMA can be systemic and has poor outcome with <20% 1-year survival (Jodele S et al. Blood 2014). These patients with severe bleeding were reported to have gastrointestinal (GI) vascular injuries. We reviewed 108 post-HSCT endoscopic biopsies from 50 patients and newly identified statistically significant histological features of iTMA.

Design: Biopsies from patients with suspected intestinal graft vs. host disease (iGVHD) were used. In addition to histological evaluation of iGVHD, we evaluated 8 criteria for iTMA (table). Patients were divided into 3 groups using current clinical criteria of iGVHD and TMA: iGVHD/TMA, iGVHD alone, and no iGVHD/no TMA. Histologic markers were scored as present or absent in a blind fashion. Statistical analysis was performed using Fisher exact test.

Results: Fifteen patients (30%) had iGVHD and TMA. Out of 35 patients without TMA, 21 had iGVHD and 14 did not. Incidence of clinically severe iGVHD (stage 3-4) was similar in TMA/iGVHD and iGVHD alone groups (79% vs 64%). Histologic signs of iTMA except for mucosal hemorrhages and endothelial swelling were statistically significant in patients with TMA. Intravascular thrombi were only seen in TMA group.

HSCT patients with diarrea (n=50)				
	TMA/iGVHD (n=15)	iGVHD alone (n=21)	No TMA/no iGVHD (n=14)	p=value
Mucosal hemorrhages	12 (80%)	11 (52.4%)	5 (36%)	0.057
Loss of glands	11 (73.3%)	8 (38%)	0 (0%)	
Intravascular schistocytes	10 (66.7%)	5 (23.8%)	3 (21.4%)	0.016
Intravascular fibrin	8 (53.3%)	2 (9.55%)	2 (14%)	0.008
Intravascular microthrombi	4 (26.6%)	0 (0%)	0 (0%)	0.010
Endothelial swelling	13 (86.6%)	13 (61.9%)	7 (50%)	0.086
Endothelial separation	8 (53.3%)	3 (14.3%)	1 (7%)	0.007
Mucosal denudation	7 (46.7%)	3 (14.3%)	0 (0%)	0.005

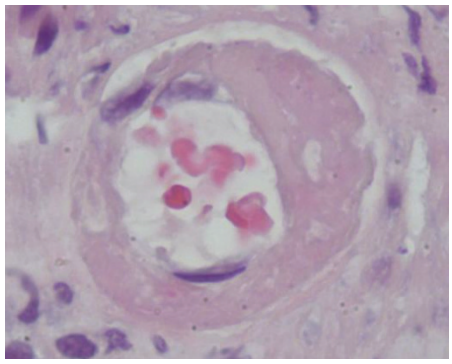

Conclusions: We identified histologic features of iTMA that are useful to delineate GI vascular injuries in post-HSCT patients. Recognition of these histological signs in patients with GI symptoms may guide early treatments for iTMA.

Pulmonary Pathology (including Mediastinal)

1890 Yield of EGFR and ALK Testing in Poorly Differentiated Non-Small Cell Lung Carcinomas

Charles Allen, Bin Yang, Carol Farver, Sanjay Mukhopadhyay. Cleveland Clinic, Cleveland, OH.

Background: Current IASLC/ATS/ERS guidelines recommend testing all non-squamous non-small cell lung carcinomas (NSCLC) for EGFR mutations and ALK translocations, including adenocarcinomas that require immunohistochemistry for subtyping and NSCLC that are unclassifiable after immunohistochemistry (NSCLC, NOS). There is no data comparing the yield of molecular testing in these groups to adenocarcinomas that are easily subtyped on H&E. The aim of this study was to compare the yield of molecular testing in adenocarcinomas that are easily classifiable on H&E to adenocarcinomas that require immunohistochemistry for subclassification, and NSCLC, NOS.

Design: Ninety-one (91) lung specimens (61 biopsies, 30 resections) with NSCLC were reviewed by a pulmonary pathologist blinded to the original diagnosis, results of immunohistochemical stains (if used) and EGFR/ALK status. Cases were separated into 3 categories: adenocarcinoma, easily classifiable on H&E, poorly differentiated adenocarcinoma (unclassifiable on H&E, but TTF-1-positive) and NSCLC, NOS (unclassifiable on H&E, and negative for TTF-1 and p63/p40). The incidence of EGFR mutations and ALK translocations in the 3 groups was compared. An additional 22 cases (18 biopsies, 4 resections) of NSCLC, NOS were retrieved from our pathology archives. Results of molecular testing in each group were reviewed.

Results: Of 91 NSCLC,13 were classified as squamous cell carcinoma on H&E and excluded.Of the remaining 78, 61 were readily subtyped as adenocarcinoma on H&E, 10 were unclassifiable on H&E but TTF-1-positive (poorly differentiated adenocarcinoma), and 7 were NSCLC, NOS. An additional 22 random NSCLC, NOS cases were added, bringing the NSCLC, NOS cases to 29. EGFR mutations were detected in 11/61 adenocarcinomas easily classifiable on H&E (18%), 1/10 poorly differentiated adenocarcinomas (10%) and 0/29 NSCLC, NOS (0%). ALK translocations were found in 2/61 easily classifiable adenocarcinomas (3%), 0/10 poorly differentiated adenocarcinomas (0%) and 2/29 NSCLC, NOS (7%). EGFR mutations were significantly less likely to be found in NSCLC, NOS than in adenocarcinomas (p=0.0168, Fisher's exact test, 2-tailed).

Conclusions: Oncogenic driver mutations (EGFR or ALK) do occur in poorly differentiated adenocarcinomas and NSCLC, NOS, although the yield of EGFR mutations is significantly lower in NSCLC, NOS when compared to adenocarcinomas. These findings support molecular testing of all non-squamous NSCLC, including poorly differentiated adenocarcinomas that require immunohistochemistry for subtyping, and NSCLC, NOS.

1891 A Novel High-Speed Droplet-Polymerase Chain Reaction Can Detect Epidermal Growth Factor Receptor Gene Mutation in Non-Small Cell Lung Cancer in Less Than 10 Minutes

Shiho Asaka, Akihiko Yoshizawa, Kazuyuki Matsuda, Akemi Yamaguchi, Yukihiro Kobayashi, Rie Nakata, Zhang Meng, Mitsutoshi Sugano, Takayuki Honda. Shinshu University Hospital, Matsumoto, Nagano, Japan; Seiko Epson Corporation, Shiojiri, Nagano, Japan.

Background: Somatic mutations in the epidermal growth factor receptor (*EGFR*) gene are associated with the response to tyrosine kinase inhibitors in patients with non-small-cell lung cancer (NSCLC). Cases of clinical urgency require the use of a rapid assay for detecting *EGFR* gene mutations. The purpose of this study was to develop a novel rapid assay for detecting *EGFR* gene mutations by using a real-time droplet-polymerase chain reaction (d-PCR) system (Seiko Epson Corporation) with formalin-fixed paraffin-embedded (FFPE) fresh bronchial lavage fluid (BLF) and fresh pleural effusion (PE) specimens.

Design: First, we selected 14 specimens from NSCLC patients with L858R mutation in exon 21, which is the most common mutation of the *EGFR* gene. Next, we attempted to confirm the mutation by direct sequencing (for seven FFPE specimens) and real-time